The necessary distance between large wind farms offshore - study

Frandsen, S.; Barthelmie, R.J.; Pryor, S.C.; Rathmann, Ole; Larsen, Søren Ejling; Højstrup, Jørgen; Nielsen, P.; Thøgersen, M.L.

Publication date:
2005

Document Version
Publisher's PDF, also known as Version of record

RISØ

Risø-R-1518(EN)

The necessary distance between large wind farms offshore - study

Sten Frandsen, Rebecca Barthelmie, Sara Pryor, Ole Rathmann, Søren Larsen, Jørgen Højstrup
Wind Energy Department
Risø National Laboratory

Per Nielsen, Morten Lybech Thøgersen
EMD

Risø National Laboratory
Roskilde
Denmark
August 2004

Author: Sten Frandsen, Rebecca Barthelmie, Sara Pryor, Ole Rathmann, Søren Larsen, Jørgen Højstrup, Per Nielsen, Morten Lybech Thøgersen
Title: The necessary distance between large wind farms offshore - study

Report number
Risø-R-1518

August 2004

ISBN: 87-550-3447-0

Executive summary

A review of state of the art wake and boundary layer wind farms was conducted. The predictions made for wind recovery distances (that might be used to estimate optimal placing of neighbouring wind farms) range between 2 and 14 km. In order to model the link between wakes and the boundary layer the new Storpark Analytical Model has been developed and evaluated. As it is often the need for offshore wind farms, the model handles a regular array-geometry with straight rows of wind turbines and equidistant spacing between units in each row and equidistant spacing between rows. Firstly, the case with the flow direction being parallel to rows in a rectangular geometry is considered by defining three flow regimes. Secondly, when the flow is not in line with the main rows, solutions are found for the patterns of wind turbine units emerging corresponding to each wind direction. The model complex will be adjusted and calibrated with measurements in the near future.

Contract no.:
Danish Public Service Obligation (PSO) funds F&U 2108.

Group's own reg. no.:
1120137-00

Sponsorship:
PSO F&U 2108

Cover :

Pages: 29
Tables: 2
References: 17

Risø National Laboratory
Information Service Department
P.O.Box 49
DK-4000 Roskilde
Denmark
Telephone +45 46774004
bibl@risoe.dk
Fax +45 46774013
www.risoe.dk

Contents

Objectives and structure

The main objective of the Storpark project was to develop methods to determine the optimal distance between large wind farms in the offshore environment. The main results are given in Section 1. An overview of the supporting work is given in Section 2 which gives brief reviews of the notes produced for this report. Section 3 gives a list of presentations, Section 4 papers and posters from the project and Section 5 a list of additional references used in this work. All are given in full on the CD.

1 Summary of main results

1.1 Executive summary

A review of state of the art wake and boundary layer wind farms was conducted. The predictions made for wind recovery distances (that might be used to estimate optimal placing of neighbouring wind farms) range between 2 and 14 km. In order to model the link between wakes and the boundary layer the new Storpark Analytical Model has been developed and evaluated. As it is often the need for offshore wind farms, the model handles a regular array-geometry with straight rows of wind turbines and equidistant spacing between units in each row and equidistant spacing between rows. Firstly, the case with the flow direction being parallel to rows in a rectangular geometry is considered by defining three flow regimes. Secondly, when the flow is not in line with the main rows, solutions are found for the patterns of wind turbine units emerging corresponding to each wind direction. The model complex will be adjusted and calibrated with measurements in the near future.

1.2 Review of models

Reviews of boundary-layer and wake models ranging in from engineering models to CFD showed a wide range of predictions for recovery of wind speed after a large offshore wind farm ranging from 2-3 km to 12-13 km. These are detailed in Section 2.1. The table below gives a summary for recovery to 98% of the free stream wind speed/power density based on a westerly transect at a wind farm based on the Horns Rev wind farm layout (72 turbines).

Model	Wind speed recovery distance (km)	Power density recovery distance (km)
WAsP z_0(block) 0.1 m	6	12
WAsP z_0(block) 0.5 m	7	12.5
WAsP z_0(block) 1.0 m	8	13
WAsP wake decay 0.075	2	-
WAsP wake decay 0.05	3	-
Added roughness: exponential z_0 decay	14 (5%-7.5)	-
Added roughness: constant z_0	14 (5%-5.5)	-
*EMD CFD model: z_0 0.1-0.5 m	8	-
*EMD CFD model: z_0 1 m	7	-

One of the main issues is that the wakes generated by the wind farm are not parameterised to interact with the boundary-layer. Hence a new model was developed which is described in the paper submitted to the EWEA. The paper is given in full in the next section and a comparison of the new model with other state of the art wake models is given in section 1.3.

1.3 Paper submitted to EWEC conference 2004

Analytical modelling of wind speed deficit in large offshore wind farms

Sten Frandsen, Rebecca Barthelmie, Sara Pryor, Ole Rathmann, Søren Larsen, Jørgen Højstrup, Morten Thøgersen1
Risoe National Laboratory,
4000 Roskilde, Denmark
email: sten.frandsen@risoe.dk

Abstract:

The method is analytical and encompasses both small wind farms and wind farms extending over large areas.
As it is often the need for offshore wind farms, the model handles a regular array-geometry with straight rows of wind turbines and equidistant spacing between units in each row and equidistant spacing between rows. Firstly, the case with the flow direction being parallel to rows in a rectangular geometry is considered by defining three flow regimes. Secondly, when the flow is not in line with the main rows, solutions are found for the patterns of wind turbine units emerging corresponding to each wind direction.
The presentation is an outline of a model complex that will be adjusted and calibrated with measurements in the near future.

Keywords: wind farm, large, efficiency, analytical, model.

1 EMD, Aalborg Denmark

1. Introduction

The engineering models presently applied for calculating production losses due to wake effects from neighbouring wind turbines are based on local unit-by-unit momentum equations, disregarding the two-way interaction with the atmosphere. Other models, which did not reach engineering relevance or maturity, predict the array efficiency of infinitely large wind farms by viewing the wind turbines as roughness elements. As a third option, attempts were made to apply CFD schemes in determining the flow field and thus the array efficiency. The CFD schemes presently lack details and are computationally uneconomic.

Here, as it is often the need for offshore wind farms, the model handles a regular array-geometry with straight rows of wind turbines and equidistant spacing between units in each row and equidistant spacing between rows.

Firstly, the case with the flow direction being parallel to rows in a rectangular geometry is considered. Counting from the upwind end of the wind farm, the model encompasses 3 regimes as illustrated in Figure 1:

- In the first regime, the wind turbines are exposed to multiple-wake flow and an analytical link between the expansion (decay) of the multiple-wake and the asymptotic flow speed deficit is derived.
- The second regime materializes when the (multiple) wakes from neighbouring rows merge and the wakes can only expand vertically upward. This regime corresponds (but is not identical) to the flow after a simple roughness change of terrain.
- The third regime is when the wind farm is “infinitely” large and flow is in balance with the boundary layer.

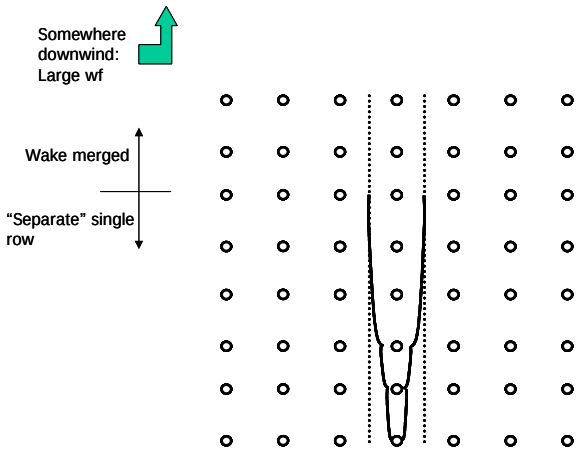

Figure 1 Illustration of the regimes of the proposed model. The wind comes from the “South”, parallel to the direction of the rows.

Secondly, when the flow direction is not in line with the main rows, solutions are found for the patterns of wind turbine units emerging corresponding to each wind direction. The solutions are in principle the same as for the base case, but with different spacing in the along wind direction and different distance to the neighbouring rows.

The regimes outlined above are discussed in detail in the following, and component models described.

2. Single wake

Initially, the flow through and around the wind turbine rotor is considered. Lanchester (1915) and Betz (1920) derived expressions that link thrust and power coefficients of the wind turbine to the flow speed deficit of its wake. The main device of these derivations were a control volume with no flow across the cylinder surface. Alternatively – and this is practical in the present context – a cylindrical control volume with constant cross-sectional area equal to the wake area and with horizontal axis parallel to the mean wind vector is defined, Figure 2. From Engelund (1968), the momentum equation in vector form for the flow volume X with the surface area A_T is

$$\int_X \rho \frac{\partial \vec{U}}{\partial t} dX + \int_{A_T} \rho \vec{U}(\vec{U} d\vec{A}) = -\int_{A_T} p d\vec{A} + \int_X \rho \vec{g} dX + \vec{T} + \int_{A_T} \vec{\tau} dA \quad (1)$$

where the acceleration term (first on the left side), the pressure term (first on the right hand side) and the gravity term (second on the right hand side) often, as is done in the following, are neglected in basic considerations. Further, the cylinder extends upwind and downwind far enough[2] for the control volume pressure to be equal to the free-stream pressure. $\vec{T}$ is the sum of forces from obstacles acting on the interior of the control volume and the last term on the right hand side is the turbulent shear forces acting on the control volume surface.

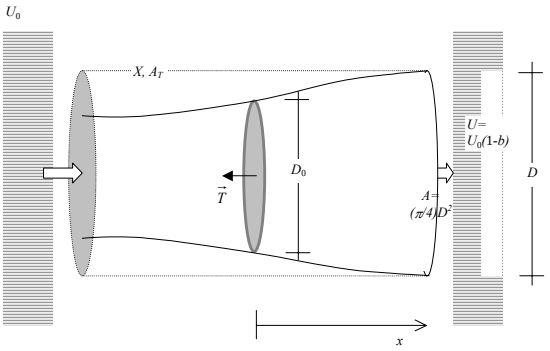

Figure 2. Control volume around a wind turbine rotor. The cylindrical control volume has the surface area A_T and volume X. The Betz control volume (full line) follows the streamlines.

Should it be acceptable to neglect shear forces in the cylinder surface and assume that pressure downwind has regained the free-stream level, the momentum equation conveniently reduces to

$$\vec{T} = -\int_{A_T} \rho \vec{U}(\vec{U} d\vec{A}) = -\int_{A_T} \vec{U} dQ, \quad (2)$$

where dQ is the volume flow out of the surface area dA. Assuming the wake to be non-turbulent, the expression can be developed further. The momentum flux out of the cylinder surface is found the following way: the volume flow (per sec.) out of the control volume's cylinder surface is equal to minus the volume flow Q_e out of the ends of the cylinder (with area $A = \pi R^2$),

$$Q_{cyl} = -Q_e = \int_A \rho U_0 dA - \int_A \rho U dA, \quad (3)$$

where U_0 is the free-flow speed and U is the flow speed in the wake. Assuming that the radius of the cylinder is sufficiently large for the flow speed in the cylinder surface to be approximated as U_0, then the momentum flux out of the cylinder surface becomes

$$M_{cyl} = U_0 \cdot Q_{cyl}. \quad (4)$$

The rotor thrust becomes

$$T = M_e + M_{cyl} \quad \Rightarrow \quad T = \int_A \rho U (U_0 - U) dA \quad (5)$$

This expression is the classical starting point for development of wake models, e.g. Engelund (1968), Schlichting (1968) and Tennekes and Lumley (1972). Next step in evaluation of the wake characteristics is to assume self-similarity of the wake flow speed profiles, i.e. the wake wind profile can be written as

$$U = U_w(x) \cdot f(r/R), \quad (6)$$

where U_w is the minimum wake flow speed, r is the distance from the center of the wake and R is a characteristic of the wake width at the distance x downwind of the rotor. Assuming the wake axis-symmetric, inserting equation (6) in (5) and introducing polar coordinates and the substitution $y = r/R$ yield

$$T = \int_0^{2\pi} \int_0^{\infty} \rho r U_w f(r/R)\left(U_0 - U_w f(r/R)\right) dr \Rightarrow$$

$$T \propto \rho R^2 \int_0^{\infty} y U_w f(y)\left(U_0 - U_w f(y)\right) dy \quad (7)$$

2 Upstream of the order ½ to 1 rotor diameter and downwind 2-3 rotor diameters.

The integral in (7) only depends on the minimum wake flow speed U_w. Therefore, equation (7) can be written as

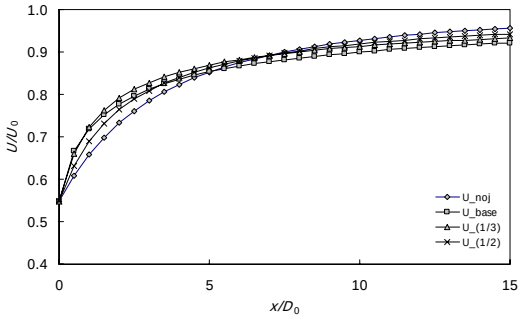

Figure 3 Comparison of single-wake models: "U_(1/2)" is the proposed mode, "U_(1/3)" is the Schlichting model, "U_noj" is Jensen (1983) model and "U_base" is Schlichting model with no linearization of momentum equation. The figure gives the relative speed in the wake as function of downwind position. C_T***=0.7,*** $2\alpha_{(noj)}$***=0.1; the flow***

$$T = C_{f1} \cdot \rho\pi R^2 U_w^{'}(U_0 - U_w^{'}), \qquad (8)$$

where $U_w^{'} = C_{f2} \cdot U_w$ is a characteristic flow speed and C_{f1} and C_{f2} are constants depending only on the integrals $\int_0^\infty f(y)dy$ and $\int_0^\infty f^2(y)dy$ i.e. the *shape* of the wake profile.

The assumption of self-similarity throughout the wake is not only questionable in general terms for the regions of the wake, which is of interest in the present context. It is definitely wrong in the near-wake region. However, the self-similarity assumption maintained in here is justified because the wake-affected wind turbine's rotor "integrates" the wake over a sizable fraction of its area, thus making the finer details less important.

Thus, any actual wake shape can be represented by a rectangular distribution of the flow speed without violating the general principles of the above derivations:

$$T = \rho AU(U_0 - U), \quad A = \frac{\pi}{4}D^2, \qquad (9)$$

where D is the diameter of the rectangular wake flow speed profile and A is the area of the wake . The thrust may also be expressed as

$$T = \tfrac{1}{2}\rho A_0 U_0^2 C_T, \quad A_0 = \frac{\pi}{4}D_0^2, \qquad (10)$$

where A_0 is the swept area of the rotor, D_0 is the rotor diameter and C_T the thrust coefficient. As pointed out previously, the derived expression is only valid some distance downwind of the rotor where the pressure has regained its free-flow value. Denominating the induction factor[3] $a = 1 - U_a / U_0$, where U_a is the flow speed in the wake after the initial wake expansion, then the thrust coefficient is related to the induction factor by

$$C_T = a(2-a) \quad \Rightarrow \quad a = 1 - \sqrt{1 - C_T}, \quad C_T < 1 \qquad (11)$$

and the wake cross-sectional area immediately after wake expansion, A_a, is related to the rotor area by

$$\frac{A_a}{A_0} = \frac{1-(a/2)}{1-a}, \qquad (12)$$

Combining equations (9), (10), (11) and (12) yields

$$A_a = \beta \cdot A_0 \text{ and } D_a = \sqrt{\beta} \cdot D_0,$$

$$\text{where} \quad \beta = \frac{1}{2} \cdot \frac{1 + \sqrt{1 - C_T}}{\sqrt{1 - C_T}} \qquad (13)$$

As indicated previously, the result applies to the wake area at the position downwind where the pressure in the wake has regained the free-flow value. In real terms, it is difficult to identify exactly that position. Here, we choose to assume that the wake expands immediately. Thus, denominating the wake area at distance x downwind from the wind turbine $A = A(x)$, the assumption is that $A(x=0) = A_a$. The assumption is crude but ensures a solution for all C_T values between 0

3 Usually, the induction factor is defined through the flow speed in the rotor plane.

and 1 of the combined equations (9) and (10), see later.
The following expression for the wake flow speed is found:

$$\frac{U}{U_0} = \frac{1}{2} \pm \frac{1}{2}\sqrt{1 - 2\frac{A_0}{A}C_T} \,. \qquad (14)$$

For $A(x{=}0) = A_a$, equation (14) has solutions for $0 \le a \le 1$, where the "+" applies for $a \le 0.5$ and "-" for $a > 0.5$. Assuming monotonous expansion of the wake for increasing x, equation (14) only has solutions for $a \le 0.5$, probably because one or more of the assumptions leading to the equation are violated. A frequently applied approximation to equation (9) for small wake flow speed deficits is $T \approx \rho A U_0 (U_0 - U)$, which in turn modifies equation (14):

$$\frac{U}{U_0} \approx 1 - \tfrac{1}{2} C_T \frac{A_0}{A} \approx 1 - a\frac{A_0}{A} \,. \qquad (15)$$

In principle this has solutions for all distances downwind and for all $0 \le a \le 1$. The above considerations allow only estimation of the initial wake flow speed deficit. In order to estimate the deficit any distance downwind, a reliable model for the wake expansion must be identified. Schlichting (1968), Engelund (1968) and others point to a solution where $D \propto x^{1/3} \Rightarrow A \propto x^{2/3}$ for $x \to \infty$. The result stems from several assumptions (most prominent constant eddy viscosity in the wake and self-similarity of the wake deficit and turbulence profiles) and is only valid in the far wake where the approximation of equation (15) is valid. Therefore – and for reasons given in the next section – it is useful to adopt a model for expansion of the wake cross-sectional area as function of distance downwind that has the form:

$$D(x) = \left(\beta^{n/2} + \alpha \cdot s\right)^{1/n} D_0, \quad s = x / D_0 \,, \qquad (16)$$

where the initial wake diameter is

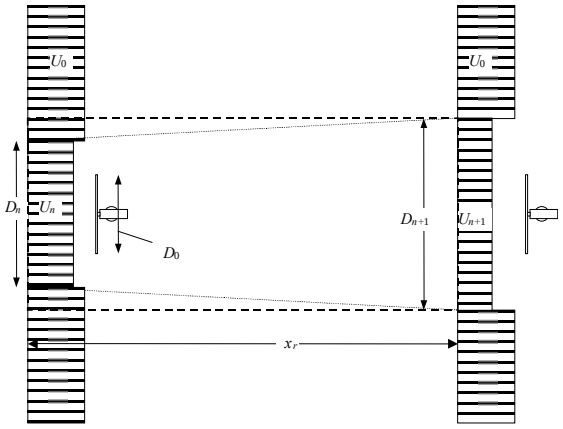

Figure 4 Flow between two units in a long row of wind turbines.

$\sqrt{\beta} \cdot D_0$. If the Schlichting solution is chosen, then n=3. The constant α must be experimentally determined. An initial estimate could be obtained by comparing Equation (15) with a model developed by Jensen (1983) and Katic et al (1986):

$$D_{(noj)}(x) = \left(1 + 2\alpha_{(noj)} \cdot s\right) D_0 \,,$$
$$\frac{U}{U_0} = 1 - a\frac{A_0}{A_{(noj)}} = 1 - a\frac{D_0^2}{D_{(noj)}^2} \qquad (17)$$

where $\alpha_{(noj)} \approx 0.1$. In this model, the initial expansion of the wake has been neglected and the linear wake expansion is presumably too large. However, being applied in the wind resource computer code WasP, the model has proven successful for wind farms of limited size. Matching the expressions (15) and (17) for wake flow speeds the distance s downwind yields

$$\left(\beta^{n/2} + \alpha s\right)^{2/n} = \beta \cdot \left(1 + 2\alpha_{(noj)} s\right)^2 \Rightarrow$$
$$\alpha = \beta^{n/2} \cdot \left[\left(1 + 2\alpha_{(noj)} s\right)^n - 1\right] \cdot s^{-1} \qquad (18)$$

Figure 3 shows the relative wake wind speed as function of downwind distance from the wake generating wind turbine for different wake shapes and with and without the linearization of equation (14).
Obviously, the decay factor depends of the distance downwind chosen to match the flow speeds. For small C_T and large s, the decay factor α is of order $10\alpha_{(noj)}$.
The square root shape (n=2) is chosen for reasons given hereafter.

3. Multiple wake, single row (regime 1)

The case of multiple-wake is dealt with as illustrated in Figure 4. Firstly, the possible effects of boundaries such as the ground and the neighboring wakes are included *implicitly* through the area growth, $dA_i = A_{n+1} - A_n$. We consider a single row of wind turbines and in that row, the wake between wind turbine no. n and wake n+1 is described, Figure 4. Outside (and in) the cylinder surface of control volume the flow speed is U_0. The wake flow-speed is assumed constant. The flow speed at the ends of the cylinder surface is denominated as indicated in Figure 4. The areas corresponding to the diameters D_* are denominated A_* and is now referring to the wind speed just in front of each unit. (note also that the cross section of the control volume need not be a circular cylinder).
Without the approximation of equation (15), we get for momentum conservation:

$$\rho A_{n+1}U_{n+1}(U_0 - U_{n+1}) = \rho(A_{n+1} - A_n)U_0(U_0 - U_0) + \rho A_n U_n(U_0 - U_n) + T \quad \Rightarrow$$

$$A_{n+1}U_{n+1}(U_0 - U_{n+1}) = A_n U_n(U_0 - U_n) + \tfrac{1}{2} A_R U_n^2 C_T \quad \Rightarrow$$

$$c_{n+1}(1-c_{n+1}) = \frac{A_n}{A_{n+1}} c_n(1-c_n) + \tfrac{1}{2}\frac{A_R}{A_{n+1}} c_n^2 C_T,$$

$$c_n = \frac{U_n}{U_0},\ c_{n+1} = \frac{U_{n+1}}{U_0} \qquad (19)$$

where

$$A_n = A_n(s) = A_n(n \cdot s_r), \quad s_r = x_r / D_0$$

is a function of the dimensionless distance s from the first wind turbine. *With* the approximation of the flow speed deficit, equation (15), the recursive equation becomes

$$c_{n+1} = 1 - \left[\frac{A_n}{A_{n+1}}(1-c_n) + \frac{1}{2} \cdot \frac{A_R}{A_{n+1}} C_T c_n \right]. \qquad (20)$$

For both approaches, a model for the wake expansion is needed.

Asymptotically for $n \to \infty$

For an infinite large number of wind turbines, $n \to \infty$, $(c_n - c_{n+1}) \to 0$, it must be assumed that there is an asymptotic, non-zero flow speed: if the flow speed becomes zero then the shear becomes zero and the flow would accelerate etc. Denominating the asymptotic value of the ratio $c_w = c_n = c_{n+1}$ for large n's, an equation for linking the asymptotic wake area and wake flow speed is obtained:

$$c_w(1-c_w) = \frac{A_n}{A_{n+1}} c_w(1-c_w) + \tfrac{1}{2}\frac{A_R}{A_{n+1}} c_w^2 C_T \quad \Rightarrow$$

$$A_{n+1} - A_n = \tfrac{1}{2} A_R \frac{c_w}{1-c_w} C_T. \qquad (21)$$

In Equation (21) the term

$\frac{1}{2} A_R \frac{c_w}{1-c_w} C_T$ is a constant, and thus – asymptotically – wake cross-sectional area is expanding linearly with x. Equation (21) points to an interesting result: With only conventional assumptions, it is possible to derive the wake expansion for an infinite row of two-dimensional obstacles (wind turbine rotors): $D \propto x^{\frac{1}{2}}$. That expansion is the only shape that asymptotically will ensure a non-vanishing and non-increasing flow speed.

By assuming the wake cross section circular, it is now possible to link the decay factor α in equation (16) to the asymptotic flow speed ratio c_1. With the wake model of equation (16) with n=2 corresponding to the square root expansion of wake diameter, the increase in wake cross section is

$$A_{n+1} - A_n = \frac{\pi}{4} D_0^2 \left(\beta + \alpha \cdot s_r \cdot (n+1)\right) - \frac{\pi}{4} D_0^2 \left(\beta + \alpha \cdot s_r \cdot n\right) = A_R \alpha \cdot s_r \quad (22)$$

where s_r is the dimensionless distance between the wind turbines in the row. Inserting equation (22) into equation (21) yields

$$\alpha = \frac{1}{2} \cdot \frac{C_T}{s_r} \cdot \frac{c_w}{1-c_w}. \quad (23)$$

Thus, if the asymptotic, relative flow speed in the wake is known, then the decay constant is given. Conversely, the relative wake flow speed is given as

$$c_w = \frac{\alpha}{\alpha + \frac{1}{2}\frac{C_T}{s_r}} \quad (24)$$

In Figure 5, the result of applying

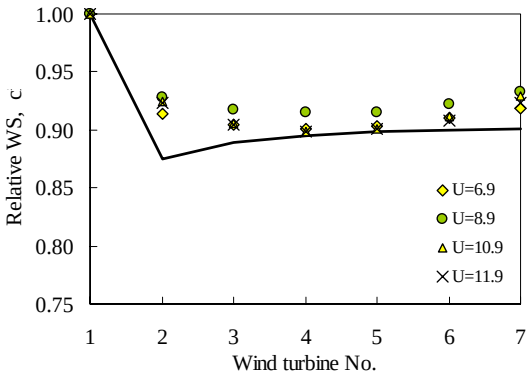

Figure 5 Measurement of wind speed ratio, c_i, at Nørrekær Enge II. Average is taken over six rows with each 7 units. $s_r \approx 7$. The wind farm consists of 42 300kW units.

equation (20) is compared with data from the wind farm Nørrekær Enge II. It is seen that the flow speed ratio (i.e. also c_w is approximately constant) is only marginally dependent on free-flow mean wind speed. With a C_T measured on a wind turbine similar to the units in question and with that curve approximated by $C_T \approx 3.5 \cdot (2U - 3.5) \cdot U^{-2}$, it is found that the decay constant must be proportional to C_T to satisfy equation (23). The full line in Figure 5 is the average of the model result for the 4 different wind speeds.

The consequence of a non-constant flow speed ratio c_w is that the decay constant α is a function of C_T, i.e. the initial wake deficit/turbulence.

4. Multiple wake, merged (regime 2)

When the wakes from different rows meet, the lateral wake expansion is stopped and the wake area can only expand upward. Since the area must expand linearly to satisfy equation (21), the height of the wake must increase linearly: this means that the growth of what is equivalent to the internal boundary layer for roughness change models asymptotically has $h \propto x$.

Also in regime 2, the "wake area" must expand linearly for the flow speed to approach a non-zero or ever increasing value. Since the wake cannot expand laterally, the incremental growth of the internal boundary layer, in regime 2, in the limit for $n \to \infty$ is

$$\Delta h = \frac{dA}{s_r D_0} = \frac{A_{n+1} - A_n}{s_r D_0}, \text{ and} \qquad (25)$$

$$\frac{\partial h}{\partial x} \approx \frac{A_{n+1} - A_n}{\Delta x} \frac{1}{s_r D_0} = \tfrac{1}{2} A_R \frac{c_{mw}}{1 - c_{mw}} C_T \frac{1}{\Delta x} \cdot \frac{1}{s_r D_0}$$

$$= \tfrac{1}{2} \frac{c_{mw}}{1 - c_{mw}} \frac{\pi}{4} D_0^2 C_T \frac{1}{s_f D_0} \cdot \frac{1}{s_r D_0} \quad \Rightarrow$$

$$\frac{\partial h}{\partial x} \approx \frac{c_{mw}}{1 - c_{mw}} c_t \Rightarrow \quad h = \frac{c_{mw}}{1 - c_{mw}} c_t \cdot (x - x_0) + h_0,$$

$$c_t = \frac{\pi C_T}{8 s_r s_f} \qquad (26)$$

where s_f is the dimensionless distance to the neighbouring rows, c_{mw} is the relative flow speed in the wake and x_0 and h_0 are integration constants to be determined. We want to make a comparison of this result with Elliott (1958):

$$h \approx \left(\frac{4}{5} z_{00}^{\frac{1}{5}} \right) \cdot x^{\frac{4}{5}}. \qquad (27)$$

For the purpose we choose the following values of the parameters:
$s_r = s_f = 7$, $C_T = 0.5$, $D_R = H = 100m$.

Where H is hub height. This gives

$$z_{00} = 0.55\text{m}, \quad \frac{\partial h}{\partial x} = 0.019$$

Further, assuming that the wake expands similarly in lateral and vertical direction from hub height, we estimate the heights of the wakes when these merge to

$$h_0 \approx H + \tfrac{1}{2} \cdot s_f D_R \approx 5 D_R \approx 500m.$$

The distance downwind from the edge of the wind farm to where the wakes merge is here estimated as:

$$x_0 \approx 10 h_0 = 5000m.$$

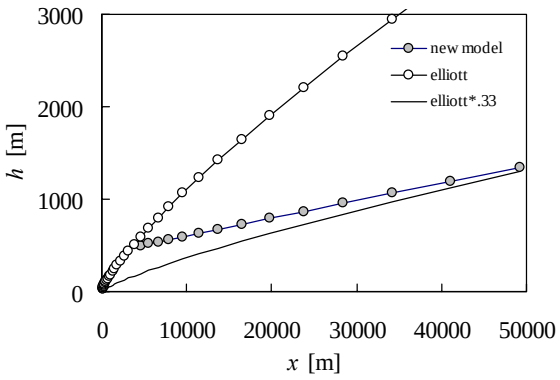

Figure 6 ***Growth of internal boundary layer as function of downwind distance to front end edge of wind farm.***

In Figure 6 the growth of the internal boundary layer is plotted for Elliott's model and for the model given by equations (26) and (27). As to the functional dependency on distance downwind, the model compares well with Elliott (1958), who suggests the approximation $h \propto x^{\frac{4}{5}}$. The Elliott model estimates the internal boundary approx. 3 times higher than the proposed model. However, the basic Elliot and Panofsky (1973) models are based on ratios of surface stress at the upstream and downstream conditions. For velocity conditions, the proper IBL height is one third of the basic height, see Sempreviva et al.(1990).
The implementation of the model is under way. Annex A describes the operationalisation of the model based on the theoretical framework described in Sections 2-5.

5. Wind farm in balance with boundary layer (regime 3)

A model for the effect of a very large wind farm on the planetary boundary layer, Frandsen (1992) and Emeis and Frandsen (1993), is outlined in the following. The first similar approach to the problem was given by Templin (1974) and Newman (1977) who – together with a few others, Bossanyi (1980) – pioneered the discipline. At the time, the approach was by most people considered far-fetched, since

wind farms extending many kilometres seemed totally unrealistic. The model presented below refines Newman (1977) by defining two flow layers divided the wind turbine hub height and by introducing the so-called geotropic drag law.

The geostrophic drag law is derived by assuming inertial and viscous forces small (low Rossby and Ekman number) relative to the Coriolis and friction forces, respectively, and pressure force. The drag law for neutral atmospheric stratification can be written as, Tennekes and Lumley (1972),

$$G = \frac{u_*}{\kappa}\sqrt{\left\{\ln\left(\frac{u_*}{fz_0}\right) - A\right\}^2 + B^2} \quad . (28)$$

Here, u_* is the friction velocity, z_0 is the surface roughness, $f = 2\Omega\sin\phi$ is the Coriolis parameter and G is the geostrophic wind speed. Ω is the angular speed of Earth and ϕ is the latitude. A and B are constants, which by Troen and Petersen (1989) are estimated to be A = 1.8 and B = 4.5. Equation (27) is implicit in u_* and for practical purposes an approximation is useful. Jensen (1978) proposed such an approximation, and with an adjustment to that approximation proposed by Emeis and Frandsen (1993), the geostrophic drag law becomes

$$G \approx \frac{u_*}{\kappa}\left(\ln\left(\frac{G}{fz_0}\right) - A_*\right) \quad \Leftrightarrow$$

$$u_* \approx \frac{\kappa G}{\ln\frac{G}{fz_0} - A_*} = \frac{\kappa G}{\ln\frac{G}{(f\cdot e^{A_*})z_0}} \quad ,(29)$$

where the constant by comparison with equation (28) is estimated to $A_* \approx 4$ at latitude 55°.

Returning to the model for the influence of the wind farm on the local wind climate, the following assumptions are made:

- The wind farm is large enough for the horizontally averaged, vertical wind profile to be horizontally homogeneous.
- The thrust on the wind turbine rotors is assumed concentrated at hub height.
- The horizontally averaged vertical wind profile is logarithmic over hub height and logarithmic under hub height. This assumption is similar to the assumption for the development of the internal boundary layer after a change of surface roughness.
- The vertical wind profile is continuous at hub height.
- Horizontally averaged turbulent wind speed fluctuations are horizontally homogeneous.
- The height of the PBL is considerably larger than wind turbine hub height: $H>>h$. Here, we could comment that forced by technology, this assumption is now only partly satisfied, depending on which boundary layer height is chosen.

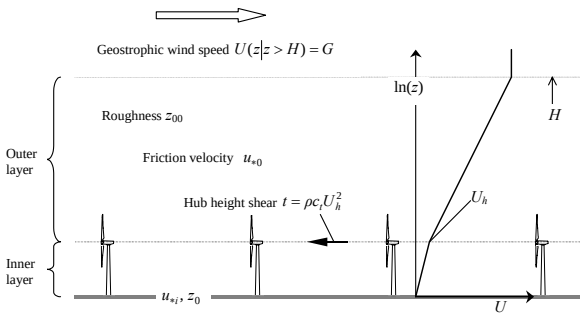

Figure 7 ***The impact of an "infinitely" large wind farm on the planetary boundary layer. The difference between G and U_h is exaggerated.***

Given that the last assumption is violated, this will be addressed further in later versions of the model.

The model for an infinitely large wind farm has to some extent been reported previously, Frandsen (1993) and Frandsen and Madsen (2003). The apparent "wind farm roughness" may be expressed as:

$$z_{00} = h\cdot\exp\left(-\frac{\kappa}{\sqrt{c_t + (\kappa/\ln(h/z_0))^2}}\right). \quad (30)$$

In particular for large wind speed deficits, this result differs significantly from Newman (1977) in that it predicts a lesser deficit. From the large-wind-farm solution the hub height wind speed and thus the flow speed ratio to the free flow speed is found, c_{wf}. The way we have built the model, this must be the asymptotic value for regime 2.

6. Other wind directions

In the regular wind turbine array is to be treated similarly: for each wind direction new rows (with larger wind turbine spacing) will form, with new (smaller) distances between rows. Merging wakes from neighbouring rows becomes a little more elaborate. For typical situations, Annex B proposes rules addition of the wakes.

7. Summary of proposed procedure

Summarizing, the model has the following components:

1. From wake 2-3 to where the wake merge with neighbour-row wakes, use "row of wts" wake shape expanding in 2 directions: $\frac{D_R}{D_1} = \frac{1}{\left(\beta_{\text{int}} + \alpha_{\text{int}} \cdot s_f\right)^{1/2}}$. The asymptotic relative wake speed deficit, $c = U/U_0$, has – if the row is long enough – an asymptotic value, c_1. The specific value is found from experiments and this value determines the decay constant α.
2. From the point of neighbour-wake merging and onward, the merged wake expands linearly upward, $h = \frac{c_{mw}}{1-c_{mw}} c_t \cdot (x - x_0) + h_0$, where x_0 and h_0 in principle is derived from the characteristics of the flow exiting regime 1.
3. Determine the relative flow speed deficit from the model from the infinitely large wind farm, c_{wf}. The first approximation is that $c_{mw}=c_{wf}$.

Apart from determining the efficiency of the wind farm, the estimation of the growth of the internal boundary layer is needed to determine what happens downwind.

8. Conclusion

Present day and near-future offshore wind farms extend 5-10 km, which in relation to the boundary layer is "large", but not "infinitely" large. Thus, there is a need for a model that handles both single and multiple wake *and* the wind farm's interaction with the atmospheric boundary layer.
It is believed that the suggested model will – with appropriate experimental "calibration" – encompass the flow characteristics of the very large wind farms in a realistic and consistent manner.

9. Future work

The model will be verified/calibrated by means of existing data and data from the large offshore demonstration project at Horns Rev and Nysted.
To verify experimentally the flow speed deficit in the infinitely large wind farm, c_{wf}, will be difficult and is presently viewed as a major challenge. Experimental data, Højstrup et al (1993), show significant speedup of the flow in between the rows, indicating that the flow is constrained already before the wake from neighbouring rows merge in the sense described above. It is believed that the proposed model can handle this by appropriate adjustments.
Presently, the model only allows simple geometries and there is a need to extend it to irregular geometries.

10. Acknowledgement

The work has in part been financed by Danish Public Service Obligation (PSO) funds.

Annex A: Implementation

The model has been operationalised ensuring that momentum is conserved at each model step (currently 1 m distance).
By utilising the equations given in the above sections, the expansion of the wake is as a circular disk (= axis-symmetric). The primary variable is the wake height. Once the wake radius (height) exceeds the hub-height, the wake is considered to have impacted the ground surface. The total momentum deficit is conserved but the area of the wake is computed by removing the below-ground portion. This occurs at approximately 10 rotor diameters (D) distance downstream of the turbine.
In the third regime when half the wake width equals the turbine spacing the neighbouring wakes merge. This occurs at ~30 D.
Again the total momentum deficit is conserved but now we remove the area below ground as before and half of the overlapping area (sector) as shown above– if the turbine is an edge turbine only one sector is removed.

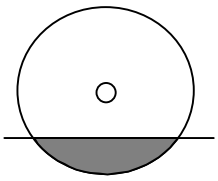

The model has been implemented using the Bonus 500 kW wind turbine thrust curve (see (Frandsen et al. 1996).) with a hub-height of 38 m and a rotor diameter of 35 m. In the case study shown in Figure 8, the freestream wind speed is 10 m and the wind farm contains 10 rows, each of 3 turbines with between and along row spacing of 300 m. Figure 8 shows the hub-height wind speed passing through the wind farm (1-3000 m) and then for a further 7000 m. In this case study the downstream wakes merge immediately with the wind farm total wake.
Figure 9 shows a close up of the first 600 m of the wind farm with two rows. The wake height increases for the first wake but then the two wakes merge

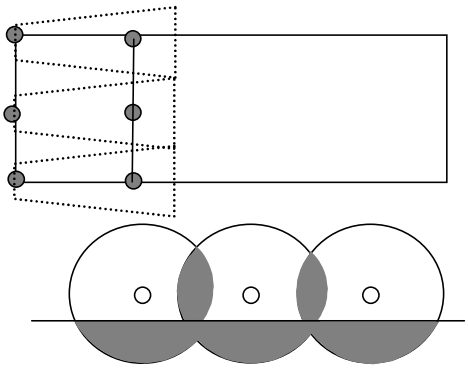

giving a rapid increase in the wake area. As shown the expansion of the single wake follows the single wake shape equation given in the 'Summary of the proposed procedure'. The double wake expansion cannot be compared directly because the total wake area for the wind farm is the area expanding in the model version. However, after the wind farm while the development of the wake height after the boundary layer follows the expansion given in equation (25) (see Figure 8).

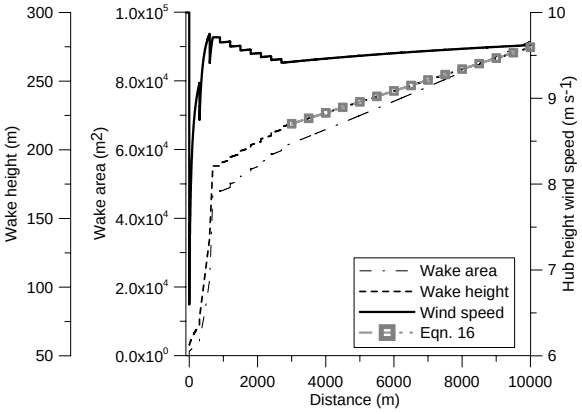

Figure 8 The model operationalised for a freestream wind speed of 10 ms^{-1} for a wind farm with 10 rows. The wake height, area and wind speed are shown for the turbine in the centre of the row.

Annex B: Merging wakes

In general

Thrust on the individual units:

$$T_1 = \int_{A_1} U_1(U_0 - U_1)dA = A_1 \cdot U_1(U_0 - U_1)$$

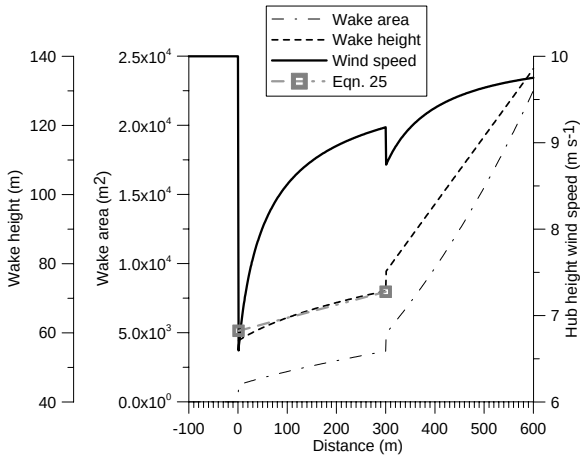

Figure 9 The model operationalised for a wind farm with 10 rows (for the first two rows). The wake height, area and wind speed are shown for the turbine in the centre of the row.

$$T_2 = \int_{A_2} U_2(U_0 - U_2)dA = A_2 \cdot U_2(U_0 - U_2)$$

Sum of thrust on the two machines:

$$T_T = T_1 + T_2 = A_1 \cdot U_1(U_0 - U_1) + A_2 \cdot U_2(U_0 - U_2)$$

I.e.:

$$A_T \cdot U_T(U_0 - U_T) = A_1 \cdot U_1(U_0 - U_1) + A_2 \cdot U_2(U_0 - U_2)$$

Where asymptotically downwind, the sum of thrust on the two machines is:

$$T_T = A_T \cdot U_T(U_0 - U_T)$$

Assume that where the wakes meet:

$$A_T = A_1 + A_2$$

Then:

$$(A_1 + A_2) \cdot U_T(U_0 - U_T) = A_1 \cdot U_1(U_0 - U_1) + A_2 \cdot U_2(U_0 - U_2) \Rightarrow$$

$$U_T(U_0 - U_T) = \frac{A_1}{A_1 + A_2} \cdot U_1(U_0 - U_1) + \frac{A_2}{A_1 + A_2} \cdot U_2(U_0 - U_2) = c \Rightarrow$$

$U_T = \frac{1}{2}U_0 \pm \sqrt{\frac{1}{4}U_0^2 - c}$, where the "+" prevails.

U_T is the integrated, initial flow speed.

A_1 and A_2 are the initial wake areas at the instance when the wakes meet.

One approach is

- to assume that U_T is the common flow speed from the point where the wakes joint, and that it develops according to the (common) wake expansion.

Another approach (and this is preferred) is

- to assume that from the point where the wakes meet, the value of U_T develops from where the wakes meet and outward and thus the two original deficits (each decreasing as were these alone) are gradually eroded according to "internal" wake expansion from the meeting point of the wakes.

By argument of momentum conservation we have $(A_1 + A_2)U_T(U_0 - U_T) = \text{constant}$ after each wind turbine.

Same thrust on two adjacent wind turbines:

If furthermore the *wakes have been generated by the same thrust*, $T = \frac{1}{2}\rho U_0^2 A_R C_T$, then

$$A_1 \cdot U_1(U_0 - U_1) = A_2 \cdot U_2(U_0 - U_2)$$

Therefore in this case

$$U_T(U_0 - U_T) = 2\frac{A_1}{A_1 + A_2} \cdot U_1(U_0 - U_1)$$

and

$$U_T(U_0 - U_T) = 2\frac{A_2}{A_1 + A_2} \cdot U_2(U_0 - U_2)$$

thus, with

$2r_1 = 2\frac{A_1}{A_1 + A_2}$ and $2r_2 = 2\frac{A_2}{A_1 + A_2}$,

we get solutions

$$U_T = \frac{1}{2}U_0 + \sqrt{\frac{1}{4}U_0^2 - 2r_1U_1(U_0 - U_1)} \quad \text{and}$$

$$U_T = \frac{1}{2}U_0 + \sqrt{\frac{1}{4}U_0^2 - 2r_2U_2(U_0 - U_2)}$$

$$U_T = \frac{1}{2}U_0 + \sqrt{\frac{1}{4}U_0^2 - 2\frac{1}{A_T} \cdot \frac{T}{\rho}} =$$

$$\frac{1}{2}U_0 + \sqrt{\frac{1}{4}U_0^2 - 2\frac{1}{A_T}\left(\frac{1}{2}U_0^2 A_R C_T\right)}$$

where A_R is the wt rotor area and $A_T = A_1 + A_2$ is the area of the summed wake.

Same length of the two wakes
Compare the above result with the individual wake:

$$U_1 = \frac{1}{2}U_0 + \sqrt{\frac{1}{4}U_0^2 - \frac{1}{A_1}\left(\tfrac{1}{2}U_0^2 A_R C_T\right)}$$

If $A_1 = A_2$, corresponding to the same length of the two wakes, then obviously $U_T = U_1 = U_2$. Thus, in this case, the joint-wake has the same deficit as the individual wakes. The same goes for many adjoining wakes, as illustrated in the figure. We get

$$U_{T(n)} = \frac{1}{2}U_0 + \sqrt{\frac{1}{4}U_0^2 - \frac{n}{\sum A_i}\left(\tfrac{1}{2}U_0^2 A_R C_T\right)}$$

$$= \frac{1}{2}U_0 + \sqrt{\frac{1}{4}U_0^2 - \frac{n}{nA_1}\left(\tfrac{1}{2}U_0^2 A_R C_T\right)}$$

$$= \frac{1}{2}U_0 + \sqrt{\frac{1}{4}U_0^2 - \frac{1}{A_1}\left(\tfrac{1}{2}U_0^2 A_R C_T\right)} = U_1$$

$$U_{T(n)} = \frac{1}{2}U_0 \cdot \left[1 + \sqrt{1 - \frac{A_R}{A_1}(2C_T)}\right]$$

References

Betz, A. (1920) Der Maximum der theoretisch mölichen Ausnützung des Windes durch Windmotoren, Zeitschrift für das gesamte Turbinenwesen, Heft 26, Sept. 26, pp. 307-309.

Bossanyi, E.A, C. Maclean, G. E. Whittle, P. D. Dunn, N. H. Lipman and P. J. Musgrove (1980) The efficiency of wind turbine clusters, Proc. Third International Symposium on Wind Energy Systems (BHRA) Copenhagen, Denmark, pp. 401-416.

Emeis, S. and Frandsen, S. (1993) Reduction of horizontal wind speed in a boundary layer with obstacles, Boundary Layer Meteorol. 64, pp. 297-305.

Elliott, W.P. (1958) The growth of the atmospheric internal boundary layer, Transactions of the American Geophysical Union 39, pp. 1048-1054.

Engelund, F.A. (1968) Hydraulik, Newtonske væskers mekanik, Den Private Ingeniørfond, Danmarks Tekniske Højskole, in Danish (Hydraulic, the Mechanics of Newtonian Fluids, thee Private Engineering Fund, Technical University of Denmark), 322 p.

Frandsen, S. (1991) On the wind speed reduction in the center of large clusters of wind turbines, Proc. of European Wind Energy Conference 1991, October, Amsterdam, Netherlands, pp. 375-380.

Frandsen, S. (1992) On the wind speed reduction in the center of large clusters of wind turbines, Jour. of Wind Engineering and Industrial Aerodynamics, 39, pp. 251-265

Frandsen, S. and P.H. Madsen (2003) Spatially average of turbulence intensity inside large wind turbine arrays, European Seminar on Offshore Wind Energy in the Mediterranean and Other European Seas (OWEMES 2003), Naples, Italy, April 10-12.

Frandsen, S., Chacon, L., Crespo, A., Enevoldsen, P., Gomez-Elvira, R., Hernandez, J., Højstrup, J., Manuel, F., Thomsen, K., and Sørensen, P. (1996). "Measurements on and modelling of offshore wind farms." *Risø-R-903(EN)*, Risø National Laboratory, Denmark.

Højstrup, J., M. Courtney, C.J. Christensen and P. Sanderhoff (1993) Full-scale measurements in wind turbine arrays. Nørrekær Enge II. CEC/Joule. Risø report I684. March.

Jensen, N. O. (1983) A note on wind turbine interaction, Risø National Laboratory, DK-4000 Roskilde, Denmark, Risø-M-2411, 16 p.

Jensen, N.O. (1978) Change of surface roughness and the planetary boundary layer, Quart. J. R. Met. Soc, No. 104, pp. 351-356.

Katic, I., J. Højstrup and N.O. Jensen (1986) A simple model for cluster efficiency, Proc. European Wind Energy Conference and Exibition, Rome, Italy, pp. 407-410.

Lanchester, F. W. (1915) Contribution to the Theory of Propulsion and the Screw Propeller, Transaction of the Institution

of Naval Architects, Vol. LVII, March 25, pp. 98-116.

Newman, B. G. (1977) The spacing of wind turbines in large arrays, J. Energy Conversion, vol. 16, pp. 169-171.

Panofsky, H. A. (1973); Tower climatology, in D. A. Haugen (ed.) Workshop on Micrometeorology, Amer. Meteorol. Soc., Boston, USA) pp. 151-176.

Schlichting, H. (1968) Boundary layer Theory, McGraw-Hill Book Company, Sixth edition.

Sempreviva, A.M., Larsen, S.E., Mortensen, N.G. and Troen, I. (1990) Response of neutral boundary layers to changes of roughness. Boundary-Layer Meteorology, 50, 205-225.

Templin, R. J. (1974); An estimation of the interaction of windmills in widespread arrays, National Aeronautical Establishment, Laboratory Report LTR-LA-171. Otawa, Canada, 23 p.

Tennekes, H. and J. L. Lumley (1972) A first course in turbulence, MIT press, Cambridge, Massachusetts, and London, England, 300 p.

Troen, I. and E. L. Petersen (1989) European Wind Atlas, Risø National Laboratory, ISBN 87-550-1482-8, 656 p.

1.4 Evaluation of the Storpark model

The new Storpark model has been compared against a number of state of the art wake models listed in the Table below.

Model owner	Name	Type
RGU	3D-NS	CFD
ECN	Wakefarm	Ainslie
UOL	FlaP	Ainslie
GH	WindFarmer	Ainslie
RISOE	Analytical	Momentum deficit
RISOE	Engineering model	Engineering
RISOE	WAsP/PARK (Version 8)	Engineering

The measured data were from an experiment using sodar at the Vindeby wind farm which gave a number of cases of single wakes at different distances from the wind turbine between 1.7 and 7.1 D. In general terms it is very difficult to prove that any of the models outperformed each other. There is also fairly high measurement uncertainty. The Storpark Analytical model typically gives results for the velocity deficit at hub-height which is in the centre to the high end of the range of the predictions by the different models. However, it is important to remember that the Storpark Analytical Model is not designed for single wake predictions. The most important evaluation will be against data from large offshore wind farms. An important part of this evaluation will be the constants used in the model to describe the wake expansion in different regimes which requires observational input.

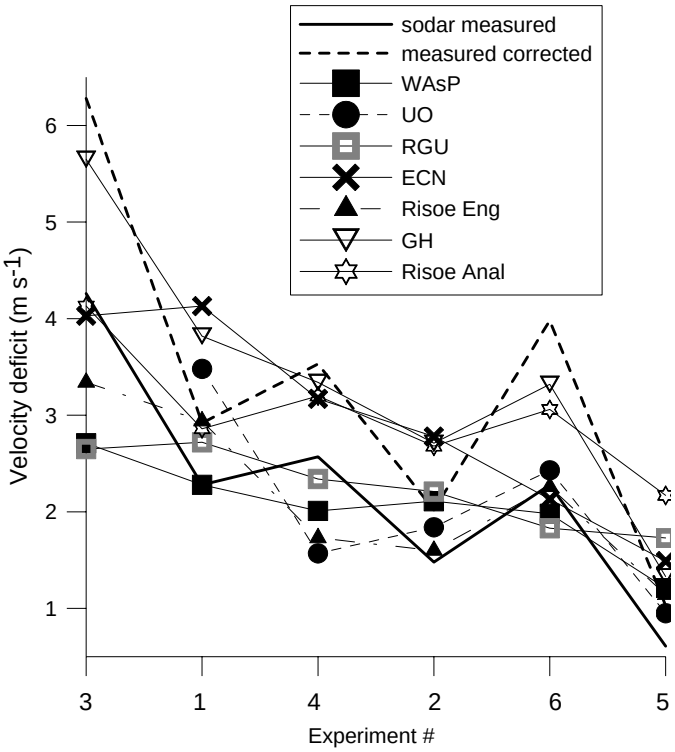

Comparison of measured and modelled velocity deficits at hub-height arranged in order of increasing distance between the turbine and the measurement point from 1.7 to 7.4D.

2. Overview of supporting work

The objectives of Storpark were:

- to review wake and boundary layer models
- to review available data
- to develop and evaluate new models
- A series of notes, presentations and papers was produced for each objective which are summarised below.

2.1. Review of wake and boundary layer models

2.1.1 WAsP8 wake effects model

Author: Ole Rathmann (Risø)
Wake effects in WAsP8 use the WAsP approach to wake calculation calculating the velocity deficit according to the thrust coefficient and the wake expansion angle. WAsP8 allows calculation of wakes from different turbines by considering the overlap area of the new wake with the upwind wake as a ratio of the overlap area with the new wake area. It does not account for terrain effects in the wake expansion.

2.1.2 Comparing WindPRO and Windfarmer wake loss calculation

Author: Per Nielsen (EMD)
The performance of the two models was compared at the Klim Fjordholme wind farm with 35 600 kW Vestas V44 wind turbines. Windfarmer appears to underestimate the wake losses in the array by about 2% relative to WindPRO. This can be altered using different Wake Decay Coefficients (or different Ct curves).

2.1.3 Overview of models and preliminary analysis

Authors: Rebecca Barthelmie and Sara Pryor (Risø)
This review includes boundary layer models – WAsP and WAsP Engineering, the Coastal Discontinuity Model, the KNMI model and mesoscale models (KAMM). The UPMPARK wind farm model is also described. The main issue is that wake models in general do not include a feedback loop describing the impact of the turbine induced changes to the boundary-layer structure. This paper also presents preliminary analysis from the Vindeby wind farm and meteorological masts and the meteorological data from Omø Stålgrunde. These data seem to indicate that the wind farm at Vindeby can be detected 2 km downwind and that the variability with different stability conditions cannot be detected, possibly due to statistical noise.

2.1.4 Strømmingsmodeller

Author: Mads Sørensen (EMD)

This review describes available boundary-layer models from mesoscale to microscale and gives web site addresses where the models can be obtained.

2.1.5 Overview of single and multiple wake models

Author: Morten Lybech Thøgersen (EMD)
This review describes the available wake models divided into i) analytical models ii) 2-d numerical models and iii) 3-d numerical models and gives references to each model. Different approaches to moving from single to multiple wakes are described.

2.2. Review of existing data

2.2.1 Vindeby analysis

Authors: Sara Pryor and Rebecca Barthelmie
Data from the Vindeby wind farm have been used to assess whether the velocity deficit or width of the wake is different from single, multiple or quintuple wakes. The wake width increases slightly from 10° in a single wake (at 8.6D) to 13 ° in a quintuple wake but it is difficult to assess whether this is significant, due to noise or possibly the definition of wake width used. Another explanation is that it is the wake directly upwind which influences the measurements. Data were also used to calculate the equivalent to WAsP's wake decay coefficient which was calculated as 0.12 – this higher value may reflect the presence of multiple wakes. Finally comparison of data collected at 1 minute and 30 minutes showed no significant differences which may imply that wake meandering is not detectable in wind speed observations in wakes.

2.2.2 Analyses on real versus calculated wind shadow

Author: Per Nielsen
Selecting data for specific directions from the Nørrekær Enge wind farms gives freestream wind directions to one mast and full wind farm shadow to the other. The power curves compare well. Significant pre processing of the data was undertaken to remove roughness, terrain and obstacle effects. After this data cleaning no clear evidence of the shadow of Nørrekær Enge 2 could be determined at a distance of 100 D but this be due to the higher turbulence at these land sites.

2.3. Development of new models

2.3.1 Wake model based on Navier stokes solution with eddy viscosity closure

Author: Morten Lybech Thøgersen (EMD)

The model is based on the Ainslie approach using eddy viscosity closure. The boundary conditions are set for the near-wake (2D) with a Gaussian velocity deficit profile and a wake width define according to the thrust coefficient Ct.

2.3.2 Wind farm modelling using an added roughness approach in WindSim CFD model

Author: Morten Lybech Thøgersen (EMD)
Using an added roughness area to represent a wind farm (here the case is Horns Rev) simulations were run with WindSim. Assuming a wind speed of 10 m/s at hub-height the recovery distance behind the wind farm (to within 2% of the freestream) was found to vary between 7.5 and 8.5 km from the last turbine in the wind farm according to the value assigned to the roughness (0.1 m to 1 m).

2.3.3 Note re: energy budget model

Author: Sten Frandsen (Risø)
The preliminary assumptions for the new wake model focused on the energy balance flowing into and out of a box around the rotor.

2.3.4 Flow field around a turbine rotor

Author: Sten Frandsen (Risø)
A more extensive discussion of the assumptions for the new wake model focused on the momentum deficit assuming a balance between the momentum flowing into and out of a cylinder and consideration of multiple wakes.

2.3.5 A new approach to multiple wake modelling

Author: Sten Frandsen (Risø)
The new approach to wake modelling is based on describing the wake expansion in three different regimes. Initially the diameter of the wake expands to the power one third, in the multiple wake situation this becomes the power one half and finally the expansion becomes wither linear or to the power fourth fifths. This was the basis for the development of the new Analytical model which is described in the EWEA paper.

2.3.6 Verification of Storpark models

Author: Morten Lybech Thøgersen
This note outlines the proposed procedure for verifying the Storpark models based on existing data sets.

3. Presentations from the project

3.1 Analytical modelling of large wind farm clusters

Authors: Rebecca Barthelmie, Sten Frandsen, Sara Pryor and Søren Larsen
This presentation was given at the international conference in Delft 'The Science of making torque from wind' and summarises the results of the project including the review of 'recovery distances' and modelling with the added roughness model.

3.2 Miscellaneous on roughness change models

Author: Sten Frandsen
This summary was given at the 3rd Storpark meeting illustrating some fundamentals from roughness change models which could be applied within the new model.

3.3 WAsP 8 wake effect modelling

Author: Ole Rathmann
At the 4th Storpark meeting a summary of how wake effects are modelled in WasP 8 was given. The biggest change from previous versions of WAsP is the possibility to include turbines with different hub-heights in the same wind farm.

3.4 Preliminary results from the SAR-wake project

Author: Charlotte Bay Hasager
The SARwake project is using satellite images to investigate wake effects at Horns Rev and a summary was given of the progress so far in Meeting 5. These illustrate that satellite derived wind speeds from Horns Rev can be used to examine the wake of the wind farm.

3.5 Roughness model, empirical analyses and wakes

Authors: Rebecca Barthelmie and Sara Pryor
This presentation focuses on the comparison of data from Vindeby and Omø Stålgrunde which indicates that WAsP may under-predict wake losses from offshore wind farms. However, the results are highly uncertain because of coastal effects on these data sets.

3.6 Vindeby_wakes

Author: Sara Pryor
Data from Vindeby indicate that at 8.6 rotor diameter distance the width and depth of wakes are not highly dependent on the number of wakes (single or multiple) present. One minute and 30 minute averaged data were compared and no differences were

found – this is taken t suggest that wake meandering is not a large influence on the measured wake.

3.7 Design of offshore wind turbines

Author: Sten Frandsen
This presentation given in Hamburg 2002 relates current design standards to state of the art modelling of the turbulence inside wind farms.

3.8 Spatially average of turbulence intensity inside large wind turbine arrays

Author: Sten Frandsen
This presentation which was the basis for the presentation at OWEMES 2003 examines models for predicting the turbulence intensity inside large wind farms and compares those with measurements e.g. from Nørrekær Enge.

3.9 Load measurements in wind farms

Author: Sten Frandsen
This presentation at NREL focuses on the need to relate modelling and measurements for load calculations inside wind farms which also incorporates extreme loads.

3.10 Background for the effective turbulence model

Author: Sten Frandsen
On overview of the state-of-the-art in fatigue load modelling and measurements using empirical models and measurements.

4 Papers and posters from this project

Title	Author	Location
Paper- 2004 EWEC	SF et al.	EWEA, London, 2004
Paper - Analytical modelling of wind speed deficit in large offshore wind farms (abstract)	SF et al.	EWEA, London, 2004
Paper - Challenges in predicting power output from offshore wind farms	RB & SP	*Journal of Energy Engineering on Sustainable Energy Systems* (submitted).
Paper - Wind energy prognoses for the Baltic region	SP/RB & JS	Baltex Meeting, Bornholm, May 2004.
Poster- Flow within and downwind of large wind farm clusters.	RB/SF/SP/SL	Nato Advanced Study Institute: Flow And Transport Processes In Complex Obstructed Geometries: From Cities And Vegetative Canopies To Industrial Problems, Kiev, May 2004.
Poster-Analytical modelling of large wind farm clusters	RB/SF/SP/SL/ MT/JM	European Geophysical Society Conference, Nice, April 2004
Paper- Historical and prognostic changes in 'a normal wind year': A case study from the Baltic	SP/RB/JS	The science of making torque from wind, Delft, April 2004
Paper - Review of wakes and large wind farms.pdf	RB/SF/SP/SL	The science of making torque from wind, Delft, April 2004
Paper (Presentation in proceedings) - Uncertainties in power prediction offshore	RB et al.	43rd Topical Expert Meeting, Skærbæk, Denmark, March 2004
Paper - Spatial average of turbulence intensity inside large wind turbine arrays	SF/PH	Offshore Wind Energy in Mediterranean and Other European Seas, Naples, April 2003.
Poster-Statistical and physical modelling of large wind farm clusters	RB/SF/SP/SL	European Geophysical Society Conference, Nice, April 2003

5 List of supporting references

Other relevant presentations, reports and papers

Jørgensen, H.E.; Frandsen, S.; Vølund, P. 2003: Wake effects on Middelgrund Windfarm. Risø-R-1415(EN) 43 p.

Højstrup et al. 1993: Full scale measurements in wind-turbine arrays. Nørrekær Enge II. Risø_I-684(EN) 30 pp. nørkærenge1.pdf + nørkærenge2.pdf

Engelund H, 1968: Excerpts from Hydrodynamik 1968.pdf

Crespo and Frandsen, 1999: Survey of modelling wakes and wind farms, Wind Energy, 2.

Hunt, J. 2002 The disappearance of laminar and turbulent wakes in complex flows, Fluid Mech. 457 (2002)

Gomez-Elvira, R. and Crespo, A. 2001: An explicit algebraic turbulent model to reproduce the aniostropy of the momentum turbulent flows in a wind turbine wake, European Wind Energy Conference

Bossanyi, E. et al. 1980: The efficiency of wind turbine clusters. Third International symposium on Wind energy Systems.

Høstrup, J. 1981: A simple model for the adjustment of velocity spectra in unstable conditions downstream of an abrupt change in roughness and heat flux, Boundary-Layer Meteorology 21.

Elliot, W.1958: The growth of the atmospheric internal boundary layer. Transactions of the American Geophysical Union 39.

Presentation on Roughness of large wind farms, SF, 2001

Frandsen, S. 2001: Vindlaster på havmøller. Presentation on Loads on offshore turbines.

Schepers, G. 2003: ENDOW : Validation and improvement of ECN's wake model.

Barthelmie et al. 2002: ENDOW workshop proceedings, Risø-R-1326(EN)

Djerf and Mattsson, 2000: Windfarm predictions & Alsvik data (FFA)

Kristensen et al. 2003: Power loss at the cutout wind speed.

Lange, B. et al. 2003: Modelling of offshore wind turbine wakes with the wind farm program FLaP, Wind Energy, 6.

Tarp-Johanssen, N.J. 2003. Extrapolation including wave loads (Presentation)

6 Acknowledgements

The work has in part been financed by Danish Public Service Obligation (PSO) funds F&U 2108.

Mission

To promote an innovative and environmentally sustainable technological development within the areas of energy, industrial technology and bioproduction through research, innovation and advisory services.

4. Vision

5. Risø's research **shall extend the boundaries** for the understanding of nature's processes and interactions right down to the molecular nanoscale.
6. The results obtained shall **set new trends** for the development of sustainable technologies within the fields of energy, industrial technology and biotechnology.
7. The efforts made **shall benefit** Danish society and lead to the development of new multi-billion industries.